JOURNAL OF GEOPHYSICAL RESEARCH, VOL. 115, A07202, doi:10.1029/2009JA014979, 2010

Click Here for Full Article

Space Technology 5 observations of the imbalance of regions 1 and 2 field-aligned currents and its implication to the cross-polar cap Pedersen currents

G. Le,[1] J. A. Slavin,[1] and R. J. Strangeway[2]

Received 9 October 2009; revised 29 January 2010; accepted 1 March 2010; published 3 July 2010.

[1] In this study, we use the in situ magnetic field observations from Space Technology 5 mission to quantify the imbalance of region 1 (R1) and region 2 (R2) currents. During the 3 month duration of the ST5 mission, geomagnetic conditions range from quiet to moderately active. We find that the R1 current intensity is consistently stronger than the R2 current intensity, both for the dawnside and the duskside large-scale field-aligned current system. The net currents flowing into (out of) the ionosphere in the dawnside (duskside) are in the order of 5% of the total R1 currents. We also find that the net currents flowing into or out of the ionosphere are controlled by the solar wind-magnetosphere interaction in the same way as the field-aligned currents themselves are. Since the net currents due to the imbalance of the R1 and R2 currents require that their closure currents flow across the polar cap from dawn to dusk as Pedersen currents, our results indicate that the total amount of the cross-polar cap Pedersen currents is in the order of ~0.1 MA. This study, although with a very limited data set, is one of a few attempts to quantify the cross-polar cap Pedersen currents. Given the importance of the Joule heating due to Pedersen currents to the high-latitude ionospheric electrodynamics, quantifying the cross-polar cap Pedersen currents and associated Joule heating is needed for developing models of the magnetosphere-ionosphere coupling.

Citation: Le, G., J. A. Slavin, and R. J. Strangeway (2010), Space Technology 5 observations of the imbalance of regions 1 and 2 field-aligned currents and its implication to the cross-polar cap Pedersen currents, *J. Geophys. Res.*, *115*, A07202, doi:10.1029/2009JA014979.

1. Introduction

[2] Field-aligned currents (FACs) form in response to the stress exerted on the magnetosphere by the solar wind and act as the primary mechanism for dissipating solar wind energy into the ionosphere and upper atmosphere during the solar wind-magnetosphere-ionosphere coupling process. As a direct manifestation of the energy deposited onto the ionosphere, the high-latitude ionosphere contains a system of Hall and Pedersen horizontal currents whose drivers are FACs. These horizontal currents flow in the ionosphere in response to the electric fields imposed on the ionosphere by the magnetosphere-ionosphere coupling. Understanding the formation of the ionospheric current systems is very important to our comprehension of the solar wind-magnetosphere-ionosphere coupling process.

[3] It is well known that the horizontal ionospheric currents at high latitudes consist of two components: (1) Pedersen currents are formed by ions flowing along the electric field and (2) $\mathbf{E} \times \mathbf{B}$ drifts drive transverse convection flows and associated horizontal Hall currents (also known as auroral electrojets), which flow transverse to the ionospheric electric field. In the case of a uniform ionospheric conductance distribution, Hall currents are divergence-free and close completely in the ionosphere by themselves. FACs are closed in the ionosphere through the curl-free Pederson currents. To date, the closure path of FACs through Pedersen currents in the ionosphere remains to be in question due to the lack of direct measurements. Traditionally, the ionospheric currents are monitored by the ground-based magnetic observations. However, ground-based magnetic observations reveal only the information about equivalent Hall currents, but the combined circuit of Pedersen currents and FACs does not produce any magnetic signature below the ionosphere and is magnetically invisible on the ground when the ionospheric conductivity is spatially uniform [*Fukushima*, 1976]. Inferring the information about Pedersen currents requires accurate knowledge of ionospheric conductance. The signature of ionospheric currents can also be directly measured above the ionosphere by polar orbiting spacecraft. However, magnetic signatures of ionospheric currents decrease with increasing altitudes and are most visible at altitudes that are rarely accessed by spacecraft with electrodynamic instruments (under ~300 km). Thus, direct mea-

[1]Heliophysics Science Division, NASA Goddard Space Flight Center, Greenbelt, Maryland, USA.
[2]Institute of Geophysics and Planetary Physics, University of California, Los Angeles, California, USA.

Copyright 2010 by the American Geophysical Union.
0148-0227/10/2009JA014979

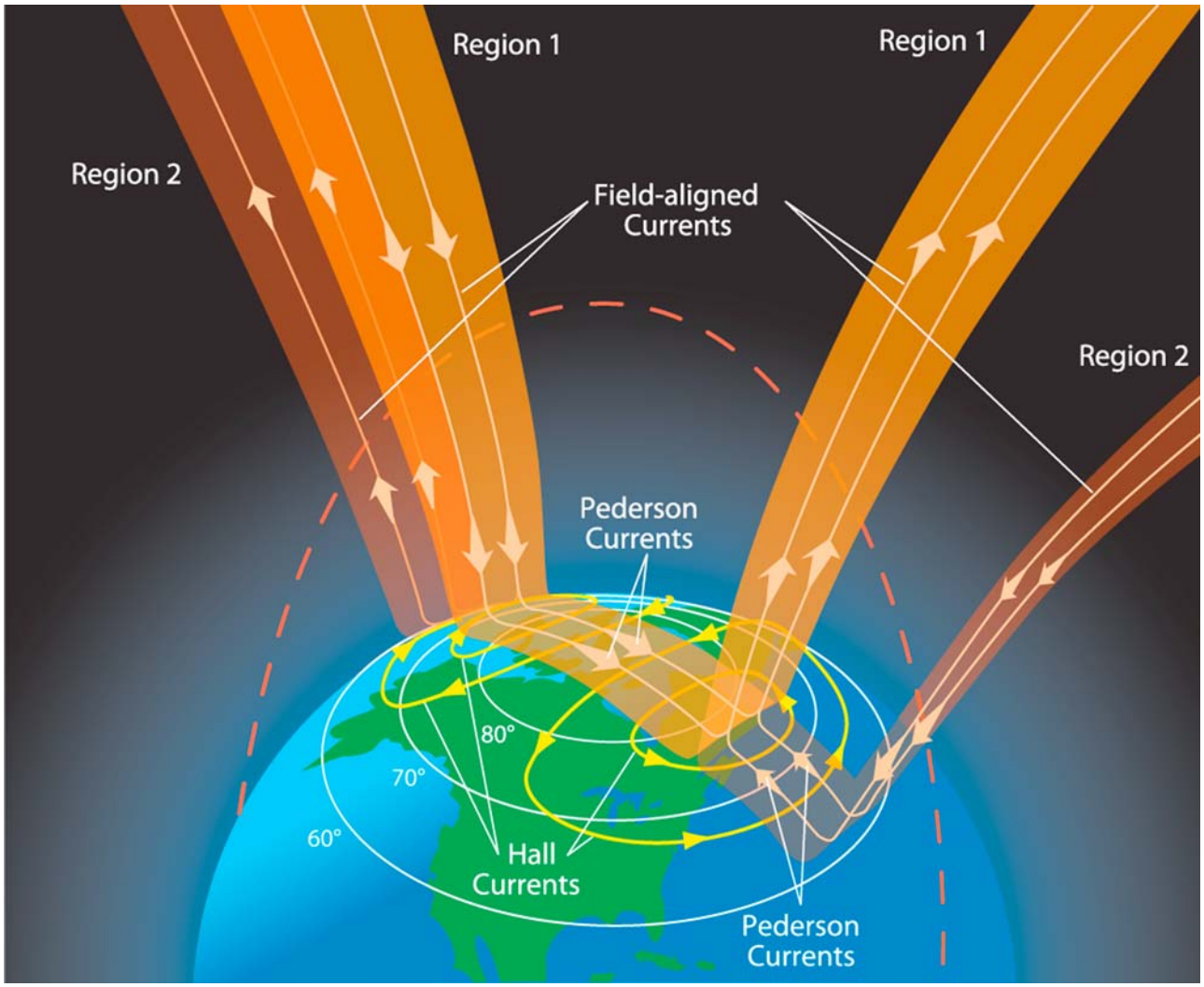

Figure 1. A schematic of combined FACs and ionospheric current systems.

surements as well as quantitative assessment of Pedersen currents have proven to be very difficult.

[4] The spatial distribution of the Pederson currents has very important space weather implications as FACs lose their energy in the ionosphere mostly through the Joule heating via Pedersen currents. It is important to understand Joule heating, because many studies have consistently established that Joule heating is the most significant process for energy inputs into the ionosphere in the high-latitude ionosphere system [*Gary et al.*, 1994; *Lu et al.*, 1995, 1998; *Fujii et al.*, 1999]. The ionosphere and upper atmosphere respond intimately to the varying energy inputs. Joule heating raises the temperature of the upper atmosphere, causing thermal expansion and changes in electron density and neutral composition [*Banks*, 1981]. Joule heating combining with solar UV radiation and ion heating by FAC-driven instabilities also cause ion outflows in the high-latitude ionosphere, which provides a significant source of magnetospheric plasma [*Chappell et al.*, 1987; *Yau and Andre*, 1997; *Strangeway*, 2000; *Zheng et al.*, 2005].

[5] Figure 1 shows a schematic of our current understanding of the combined FACs and ionospheric current systems. Here we focus on large-scale region 1 (R1) and region 2 (R2) field-aligned currents near the dawn-dusk plane and associated Hall currents and Pedersen currents. The field-aligned current near the dayside cusp region and the substorm current wedge are not a topic in this paper. Near the dawnside (dusk) auroral oval, region 1 FACs flow into (out of) the ionosphere at the high-latitude edge of the oval, which originate from the magnetopause; region 2 FACs flow out of (into) the ionosphere and map to the ring current region in the inner magnetosphere. In the ionosphere, Pederson currents flow equatorward (poleward) at the dawnside (duskside) auroral zone between the ionospheric footprints of R1 and R2 FACs to form a closed current loop. Hall currents are not part of the closure currents for FACs. Also known as auroral electrojets, they flow westward (eastward) in the dawnside (duskside) auroral oval and close in the ionosphere by flowing sunward over the polar cap to form current loops.

[6] To maintain their divergence-free condition in the combined FACs-Pedersen currents, Pedersen currents must be consistent to the net FACs flowing into or out of the ionosphere, and the overall downward FACs must eventually balance the overall upward FACs in the closed current circuit. Most of the current closure takes place via local Pedersen currents within the auroral zone flowing between the upward and downward FACs. However, observations show that there is generally an imbalance in total currents between the pair of opposite flowing R1 and R2 FACs in either dawnside or duskside, i.e., the total current flowing in R1 FCAs is more than that in R2 FACs [*Iijima and Potemra*, 1976; *Sugiura and Potemra*, 1976; *Fujii et al.*, 1981, 1994; *Stauning and Primdahl*, 2000; *Fujii and Iijima*, 1987; *Nakano et al.*, 2002; *Nakano and Iyemori*, 2003; *Christiansen et al.*, 2002]. Thus, there are net currents into (out of) the ionosphere due to the R1-R2 imbalance in the dawnside (duskside) auroral region. Such net currents need to be closed within the R1 FACs on either side of the polar cap via cross-polar cap Pedersen currents, as shown in Figure 1. *MacDougall and Jayachandran* [2008] estimated the magnitude of the cross-polar cap Pedersen currents by using the ground-based ionosonde and magnetometer observations from a polar cap station in a winter case study. They found that the total cross-polar cap Pedersen currents are ~5% of the total region 1 currents in that particular case. To our knowledge, there are no other studies focusing on quantifying the cross-polar cap Pedersen currents.

[7] The purpose of this paper is to determine the magnitude of the cross-polar cap Pedersen currents using the in situ magnetic field measurements from Space Technology 5 (ST5) mission. ST5 is a three-microsatellite constellation deployed into an elliptical (300 km perigee and 4500 km apogee), dawn-dusk, Sun-synchronous polar orbit from 22 March to 21 June 2006, for technology validations [*Slavin et al.*, 2008]. Each spacecraft carried a miniature triaxial fluxgate magnetometer and returned high-quality magnetic field data for the study of field-aligned currents [*Le et al.*, 2009]. The final calibrated magnetic field data have achieved the accuracy of better than 0.1° in pointing knowledge and 0.1% in field strength. Herein, we quantify the imbalance of regions 1 and 2 FACs using ST5 in situ magnetic field data and determine what portion of R1 currents is available to flow across the polar cap as cross-polar cap Pedersen currents.

2. Expected Magnetic Field Signatures due to R1-R2 FAC Imbalance

[8] We now use a simplified model to calculate the magnetic field perturbations expected from the combined field-aligned current-Pedersen current system. First, we consider a pair of balanced FAC current sheets (extending up above the ionosphere infinitely) and their ionospheric closure currents. On the basis of Fukushima's theorem [*Fukushima*, 1976], the magnetic field well above the ionosphere from this combined FAC-Pedersen current system is equivalent to that from two infinite FAC sheets that extend to infinity in both up and down directions. By applying Ampere's law, it is well known that the magnetic field within the two balanced, uniform, and infinite current sheets has a field strength, which is proportional to the current intensity, i.e., $B_y = \mu_o J_z$, where J_z is the current intensity or the total current per unit length along the current sheet.

[9] Now we consider three pairs of balanced infinite current sheets to model the two pairs of unbalanced current sheets, as shown in Figure 2a. In Figure 2a, the simplified geometry is such that the X direction is from dawn to dusk with the magnetic pole at $X = 0$, Z is vertically up along the magnetic pole, and Y points into the paper, westward (eastward) in the dawnside (duskside). The infinite planar current sheets are in the YZ plane with current flowing directions shown as arrows in Figure 2a. The three pairs of balanced current sheets in Figure 2a (left) are equivalent to the two pairs of unbalanced current sheets in Figure 2a (right). We can easily calculate the magnetic field generated by the three pairs of balanced infinite currents sheets. We assume the current density distribution in each infinite current sheet is in the form:

$$j_z(x) = j_o \exp(-|x - x_o|/L), \tag{1}$$

where x_o is the center location of the current sheet and j_o and L are the characteristic current density and the thickness of the current sheet, respectively. By integrating the current density j_z from $-\infty$ to $+\infty$ along the X direction, we can get the current intensity J_z of the current sheet or the total current per unit length of the current sheet along the Y direction: $J_z = 2j_o \cdot L$.

[10] In Figure 2b, we first calculate the magnetic field from two pairs of balanced R1-R2 currents on each side of the pole using characteristic current properties. The current density distribution j_z as a function of X is shown in the left panel of Figure 2a. We also list the current intensity J_z by integrating j_z over X for both R1 and R2 currents. In this case, the R1 and R2 are balanced and the net current on either side of the magnetic pole is 0. The calculated magnetic field is shown in Figure 2b (right), which is the well-known unipolar bump in the azimuthal direction (the Y direction) on either side of the magnetic pole. The magnetic field is mainly confined within the R1-R2 current sheets and quickly decreases to zero away from the current pair, both over the pole and equatorward from the R1-R2 currents.

[11] Next, we decrease the current intensity of the R2 current by 25% so that the R1-R2 currents are imbalanced, as shown in Figure 2c (left). The net current flowing into (out of) the ionosphere is 25% of the total R1 current in the dawnside (duskside). The magnetic field signature of the imbalanced R1-R2 currents is shown in Figure 2c (right). The magnetic field within the R1-R2 circuit remains to be unipolar with reduced magnitude. However, there appears to be a magnetic field offset over the pole between the dawnside and duskside FACs. The circuit of the two net current sheets in the dawnside and duskside determines the amplitude of the magnetic field offset. If we further decrease the R2 current intensity so that the net current is 50% of the total R1 current, the magnetic field offset over the polar cap also increases, as shown in Figure 2d. Thus, the signature of the imbalanced R1-R2 pairs is the magnetic field offset over the polar cap. Although the actual FACs and ionospheric current systems are much more complex than this simple model illustrates, it demonstrates the type of magnetic signatures and their magnitudes we expect to observe in situ. Using this offset, we can quantify the R1-R2 imbalance.

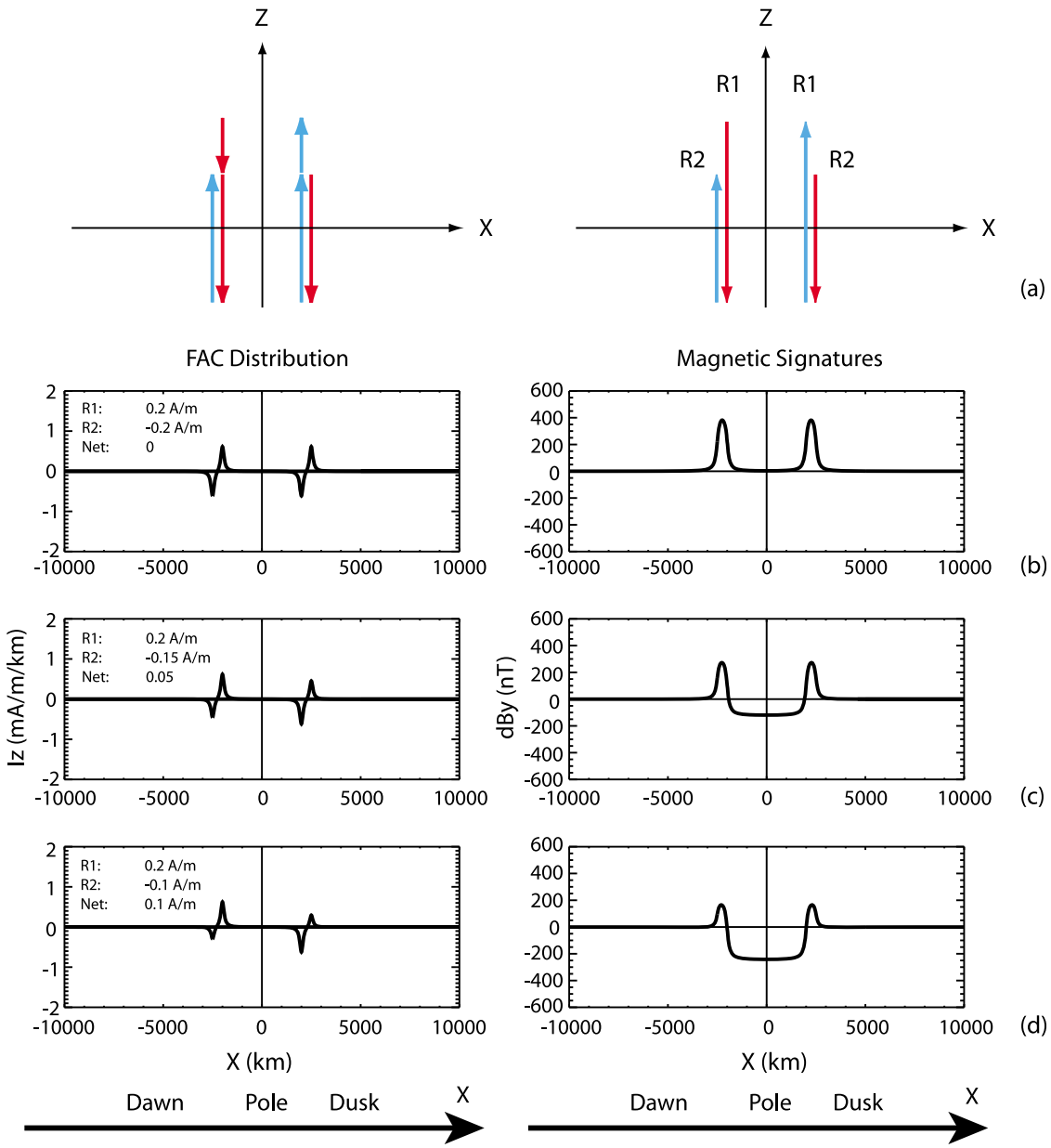

Figure 2. The FAC current setup and geometry for simple calculations of the magnetic field signatures. The polar ionosphere is simplified as a planar surface in the *XY* plane. The R1 and R2 FACs are simplified as infinite planar current sheets flowing in the vertical *Z* direction. (a) Three pairs of (left) balanced infinite current sheets to model the two pairs of (right) unbalanced current sheets. (b–d) Current (left) density distributions and their (right) magnetic field signatures.

This allows us to study the R1-R2 imbalance using in situ magnetic field observations from polar-orbiting spacecraft.

3. ST5 Observations

3.1. Data Section

[12] In this study, we use the magnetic field observations from Space Technology 5 mission to study the R1-R2 imbalance. The ST5 constellation orbits the Earth in a polar 300 × 4500 km, 105.6° inclination, Sun-synchronized orbit in the dawn-dusk meridian. The orbit period is 136 min, and the spacecraft orbit the Earth more than 10 times per day. The mission started on 22 March 2006 and lasted for 90 days. Since the Earth's rotation axis is 23.5° from ecliptic north and the Earth's magnetic pole is tilted about 11° from the rotation axis, the spacecraft orbit track across the polar cap is at a wide range of latitudes from the magnetic pole during the course of 1 day, reaching from near the magnetic pole to as low as subauroral latitudes. As we will describe next, we only select the in situ observations from those orbits with the highest latitude of the day for simplicity of the geometry. For all the selected orbits, the spacecraft cross the polar cap within 10° from the magnetic pole.

[13] There are two polar cap crossings in each ST5 orbit, one over the northern polar cap near the perigee and the other over the southern polar cap near the apogee. Near the

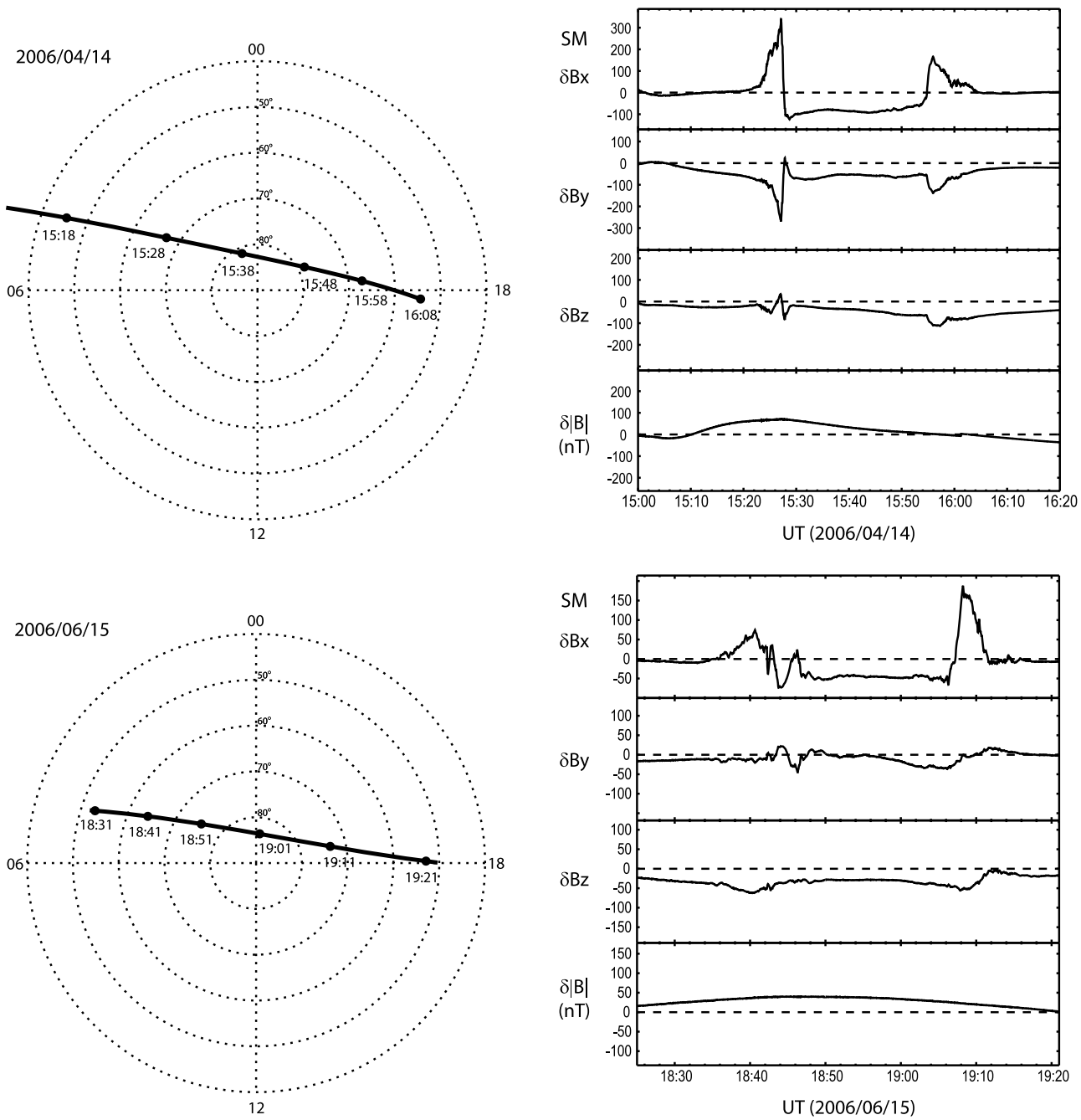

Figure 3. Examples of the magnetic field data from two selected ST5 polar cap crossings.

perigee altitudes (<500 km), the magnetic field signatures of the ionospheric horizontal currents are still visible in the magnetic field data [*Le et al.*, 2009]. They include signatures of both Hall currents and the boundary effect of the FAC-Pedersen current circuit. Since we use the infinite current sheet solutions to model the magnetic field signature of the FAC-Pedersen current system as described in the previous section, we also limit our data selection to polar cap crossings over the southern polar cap near the apogee. At these altitudes, the magnetic field due to Hall currents is invisible.

[14] During the 90 day ST5 mission, we have selected 85 polar cap crossings that have magnetic field data available from any one of the three spacecraft. The three spacecraft in the ST5 constellation are in a string of pearls configuration and the large along-track separation from the leading and the trailing spacecraft is ~5000 km or ~10 min time lag. In this paper, we use the data from one of the three spacecraft for each polar cap crossing and do not identify the specific ST5 spacecraft for the data. This is because we focus on total currents flowing within the large-scale R1 and R2 FACs instead of the structures within these currents. Figure 3 shows

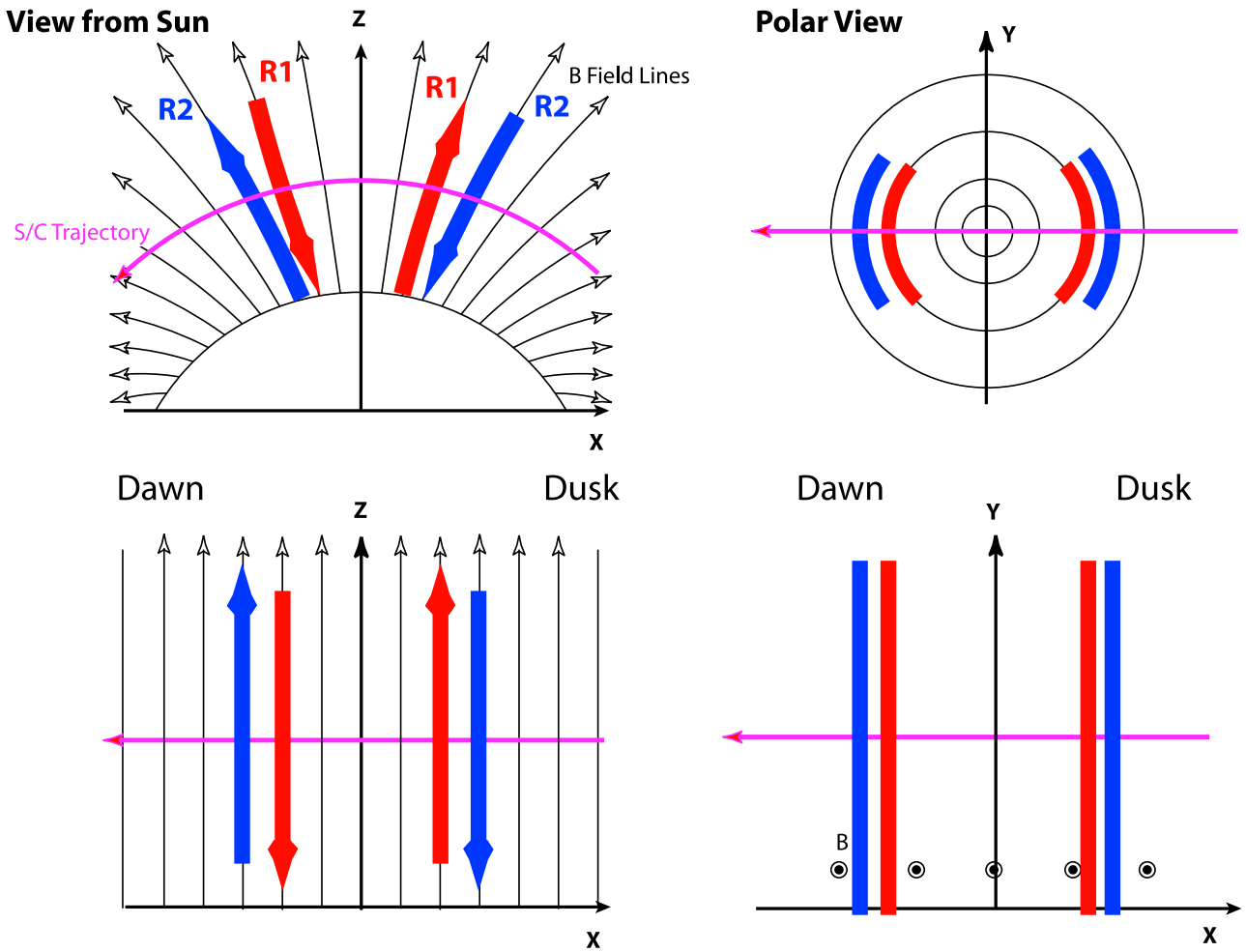

Figure 4. Simplifications of the geometry for the calculation of the total current intensity using the magnetic field observations. The top shows the realistic geometry of the ionosphere, magnetic field lines, FACs, and the spacecraft trajectory. The bottom shows the simplified geometry from the same perspectives.

two examples of the magnetic field data from the selected polar cap crossings. The spacecraft trajectories are shown in Figure 3 (left), in which we have mapped the spacecraft positions to their ionospheric footprints at 110 km altitude along the magnetic field lines. The nested circles represent constant magnetic latitudes separated by 10° and centered at the southern magnetic pole. The spacecraft move from dawn to dusk across the polar cap near the dawn-dusk meridian plane.

[15] Figure 3 (right) shows an overview of ST5 magnetic field variations generated by the field-aligned currents during these two passes, including the three components of the magnetic field residual vector (data with the internal IGRF model magnetic field removed) in the solar magnetic (SM) coordinate system, as well as the residual of the magnetic field strength. The magnetic field data shown in Figure 3 have a time resolution of 1 s, which are spin-averaged data with overlapped averaging windows. From both the examples, it is very clear that there are indeed magnetic field offsets across the polar cap, indicating that the R1 currents are stronger than the R2 currents and there are net currents flowing into or out of the ionosphere.

3.2. Data Analysis

[16] In order to quantify the imbalance of the R1-R2 FACs, we calculate the total current intensity using the magnetic field observations. We have made a few simplified assumptions in the calculations as shown in Figure 4. Figure 4 (top) shows the realistic geometry of the magnetic field lines and the ionosphere. Figure 4 (top left) is the front view from the Sun, and Figure 4 (top right) is the polar view. Traditionally, the large-scale R1 and R2 current sheets are commonly regarded as infinite sheets locally aligned with the circle of constant magnetic latitude (L shell alignment) in analyzing the magnetic field data. Figure 4 (bottom) shows the simplified geometry from the same perspectives. The X axis is along the orbit track, and $X = 0$ is the point where the spacecraft is closest to the magnetic pole. The Y axis is the cross-track direction and the Z axis vertically up along the magnetic field direction in the southern polar cap. The assumptions made for the simplification are a flat ionosphere, vertical magnetic field lines, infinite planar current sheets, and a straight orbit track through the magnetic pole.

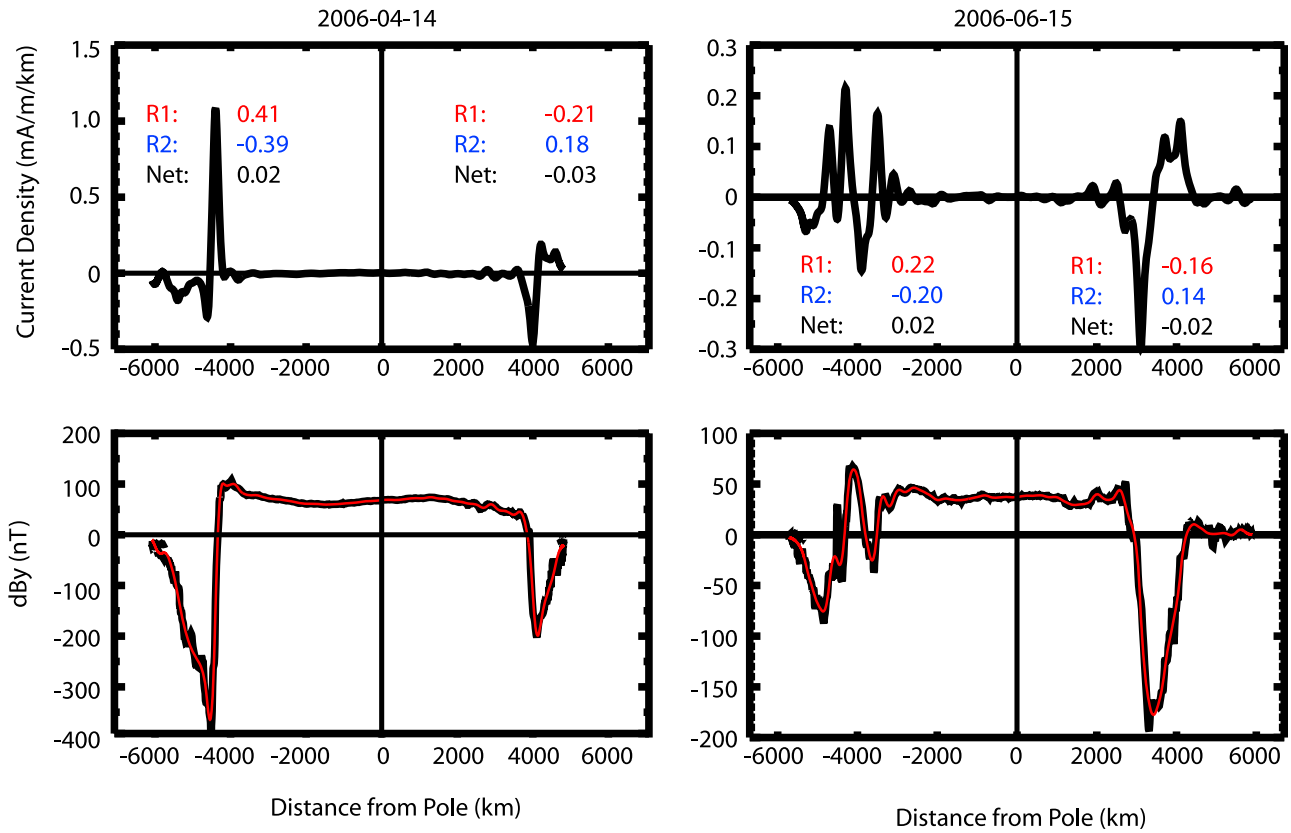

Figure 5. The least squares fit results for the two examples in Figure 4. The top shows the best fit current density distribution along the orbit track. The bottom shows the magnetic field signatures of these currents. The red traces are the best fit magnetic fields, and the black traces are the observed magnetic fields in the cross-track direction along the Y axis.

[17] Using this simplified geometry, we can derive the current intensity using the magnetic field data. We place a number of infinite current sheets in the form of equation (1) with the characteristic thickness of L = 100 km along the X axis, and the spacing between the current sheets is 200 km. The current density for the nth current sheet centered at location $x_o(n) = 200 \cdot n$ can be expressed as

$$j_z(x,n) = j_o(n)\exp(-|x - x_o(n)|/100),$$

where the characteristic current density for the nth current sheet $j_o(n)$ can be determined by fitting the data using least squares fit technique. In doing so, we calculate the magnetic fields generated by these infinite current sheets. Consider the nth current sheet first, the total current intensity integrating from $x = -\infty$ to $x = +\infty$ is

$$Jz(n) = 2j_o(n) \cdot 100.$$

The total current intensity integrated from $x = -\infty$ to x is

$$Jz(x,n) = \begin{cases} j_o(n) \cdot 100 \cdot \exp[-(x - x_o(n))/100] & x < x_o(n) \\ j_o(n) \cdot 100 \cdot [2 - \exp[-(x - x_o(n))/100] & x > x_o(n). \end{cases}$$

Thus, the contribution of the nth current sheet to the magnetic field at x, $dB_y(x, n)$, can be easily calculated based on the two infinite current sheets, one in the range $(-\infty, x)$ and the other $(x, +\infty)$. The total magnetic field at x is the sum of the contributions from all the individual current sheets:

$$B_y(x) = \sum_{n=1}^{N} dB_y(x,n),$$

where N is the total number of current sheets. The magnetic field profile $B_y(x)$ is determined by the set of $j_o(n)$. When we fit the calculated $B_y(x)$ with the observed magnetic field profile in the cross-track direction (the Y axis), the least squares fit technique will give us a set of best fit $j_o(n)$, which collectively produce the best fit magnetic field. This approach enables us to focus on FACs with scale length greater than 100 km and avoid very strong small-scale current filaments embedded within the large-scale FACs.

[18] Figure 5 shows the least squares fit results for the two examples presenting in Figure 3. Figure 5 (top) shows the best fit current density distribution along the orbit track, which is the sum of the current density from all the current sheets. Figure 5 (bottom) shows the magnetic field signatures of these currents. The red traces are the best fit magnetic fields produced by the best fit current distributions in Figure 5 (top). The black traces are the observed magnetic fields in the cross-track direction along the Y axis. It is

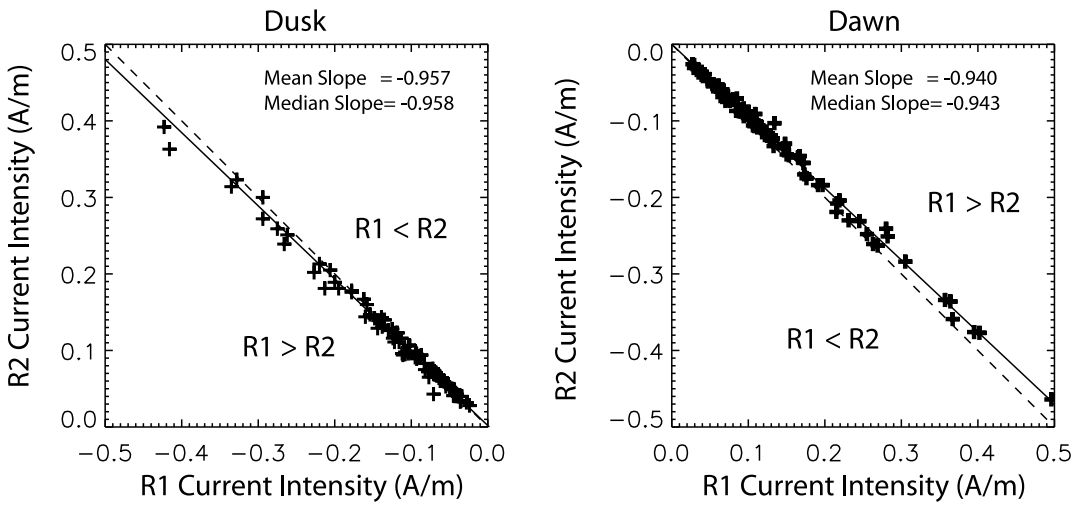

Figure 6. Statistic results of the R2 current intensity versus the R1 current intensity. The solid line has a slope, which is the average of the R2 intensity to R1 intensity ratio. The dashed line has a slope of 1.

evident that the best fit magnetic fields track the large-scale magnetic field variations in the data very well.

[19] With the best fit current density distribution, we can determine the total upward and downward current intensity in both sides of the magnetic pole by integrating current density along the *X* axis. The values of the current intensity are listed in Figure 5 (top). In the dawnside (duskside), we denote the overall downward currents as R1 (R2) and upward currents as R2 (R1). The results show a net currents flowing into (out of) the ionosphere in the dawnside (duskside). The net currents are in the order of 5%–15% of the total R1 currents in these two examples. The net current intensity into the ionosphere in the dawnside is similar to the net current intensity out of the ionosphere in the duskside.

3.3. Statistical Results

[20] We analyze the data from the entire 85 polar cap crossing selected for this study and present the statistical results here. Figure 6 shows the scatter plot of the R2 current intensity versus the R1 current intensity in the duskside and dawnside, respectively, for all these events. In each panel, the solid line has a slope which is the average of the R2 intensity to R1 intensity ratio. The mean ratio is found to be very close the median ratio, as their values are listed in Figure 6. The dashed line has a slope of 1, where the R1 and R2 currents have the same intensity. In both the dawnside and the duskside, almost all the data points are located in one side of the dashed line, where the R1 currents are stronger than the R2 currents. The net currents, due to this R1-R2 imbalance, are about 5% of the R1 currents on average in both sides of the pole.

[21] We examine the correlations between the net currents and the interplanetary magnetic field (IMF) as well as geomagnetic conditions. Figure 7 shows the intensity of the net currents as a function of IMF Bz, the Dst* index (the Dst index corrected by the solar wind dynamic pressure), and the Kp index. Figure 7 (top) is for the net upward currents in the duskside, and Figure 7 (bottom) is the net downward currents in the dawnside. The red traces represent the median values of the data points in each bin, with the bin sizes 2 nT for IMF Bz, 20 nT for Dst, and 1 for Kp index, respectively. In Figure 7 (left), the dependence of the net current intensity on the IMF Bz component displays the familiar effect of the magnetosphere's half-wave rectifier of the interplanetary electric field [*Burton et al.*, 1975]. The net current intensity increases with the increasing magnitude of the IMF Bz component for southward IMF only. Under northward IMF condition, the net current intensity is very small and does not appear to change with the IMF Bz magnitude. The effect of the magnetosphere's half-wave rectifier was first observed in geomagnetic disturbances [*Burton et al.*, 1975]. This implies that the net current intensity would be correlated with the geomagnetic indices. Figure 7 (middle and right) shows that this is indeed the case. The net currents intensify as the Dst* index becomes more negative (as the ring current indentifies) and the Kp index increases (as the global level of geomagnetic activity is enhanced). These correlations indicate that the net currents are controlled by the solar wind-magnetosphere interaction. They are enhanced during periods of enhanced interaction.

[22] Our data base also enables us to quantify readily how the FAC current intensity changes as a function of the IMF Bz and the geomagnetic indices. Figure 8 presents the R1 current intensity as a function of the IMF Bz, the Dst* index, and the Kp index, respectively. The dependence of the R2 intensity would be similar as the ratio of R2/R1 intensity is nearly constant at ~95% as shown in Figure 9. In Figure 8 (left), the R1 current intensity exhibits the effect of the magnetosphere's half-wave rectifier of the IMF Bz, i.e., it increases with the increasing magnitude of the IMF Bz component for southward IMF only. Consequently, the R1 intensity also increases as the Dst* index becomes more negative (middle) and the Kp index increases (right). These observations explain the results in Figure 7 that the net current intensity shows similar dependence on the IMF Bz and the geomagnetic indices. The enhanced net current

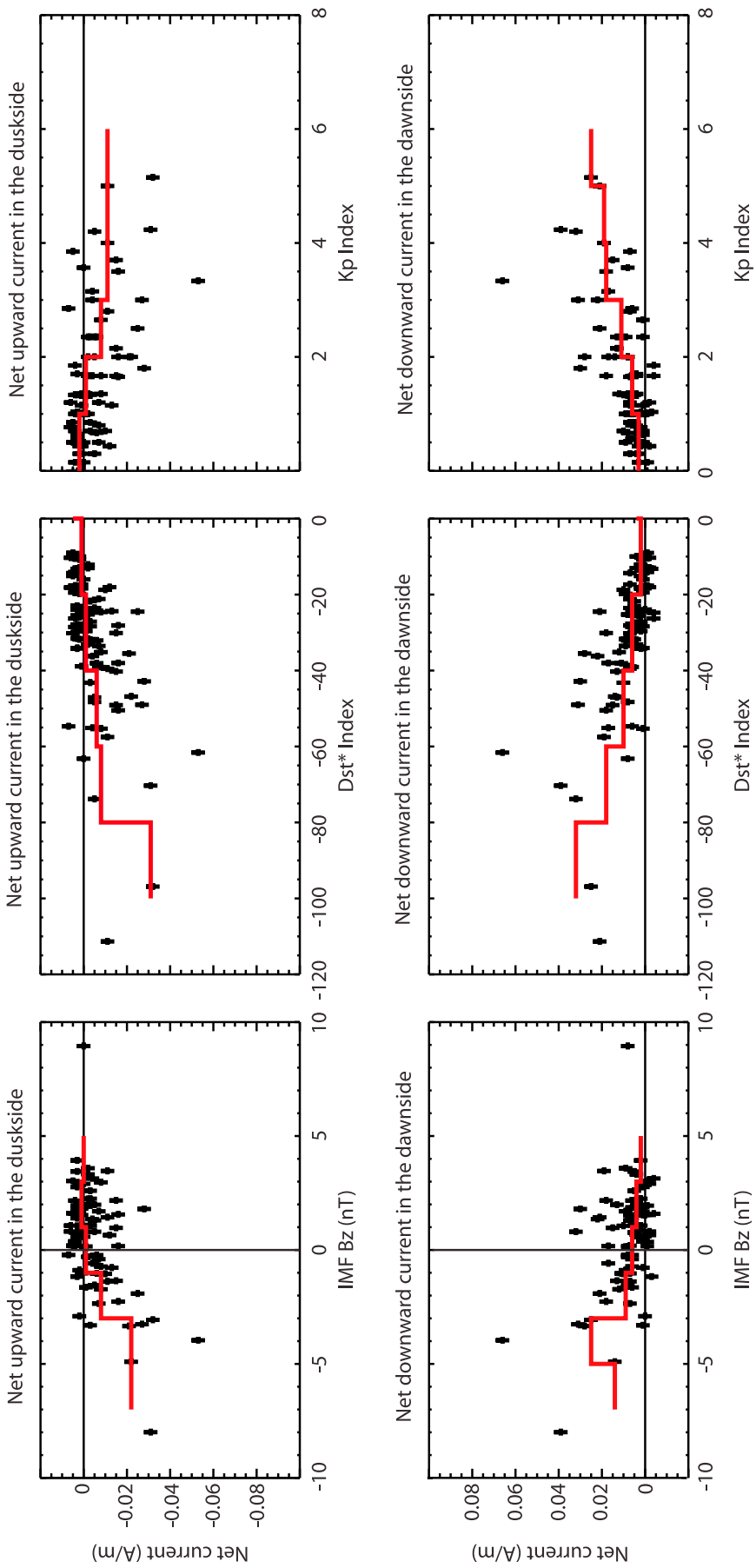

Figure 7. The intensity of the net currents as a function of IMF Bz, the Dst* index (the Dst index corrected by the solar wind dynamic pressure), and the Kp index.

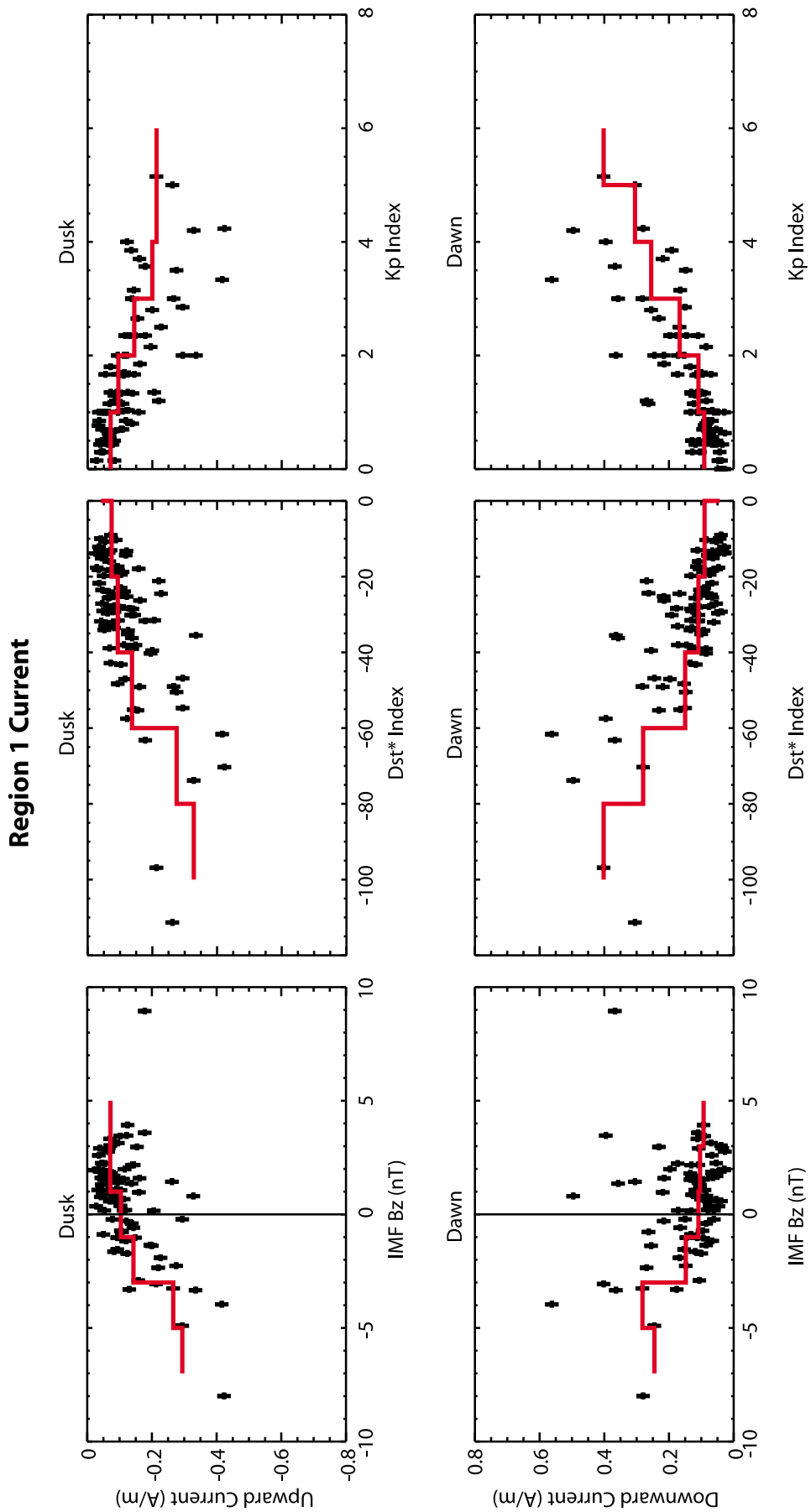

Figure 8. The intensity of the R1 currents as a function of IMF Bz, the Dst* index (the Dst index corrected by the solar wind dynamic pressure), and the Kp index.

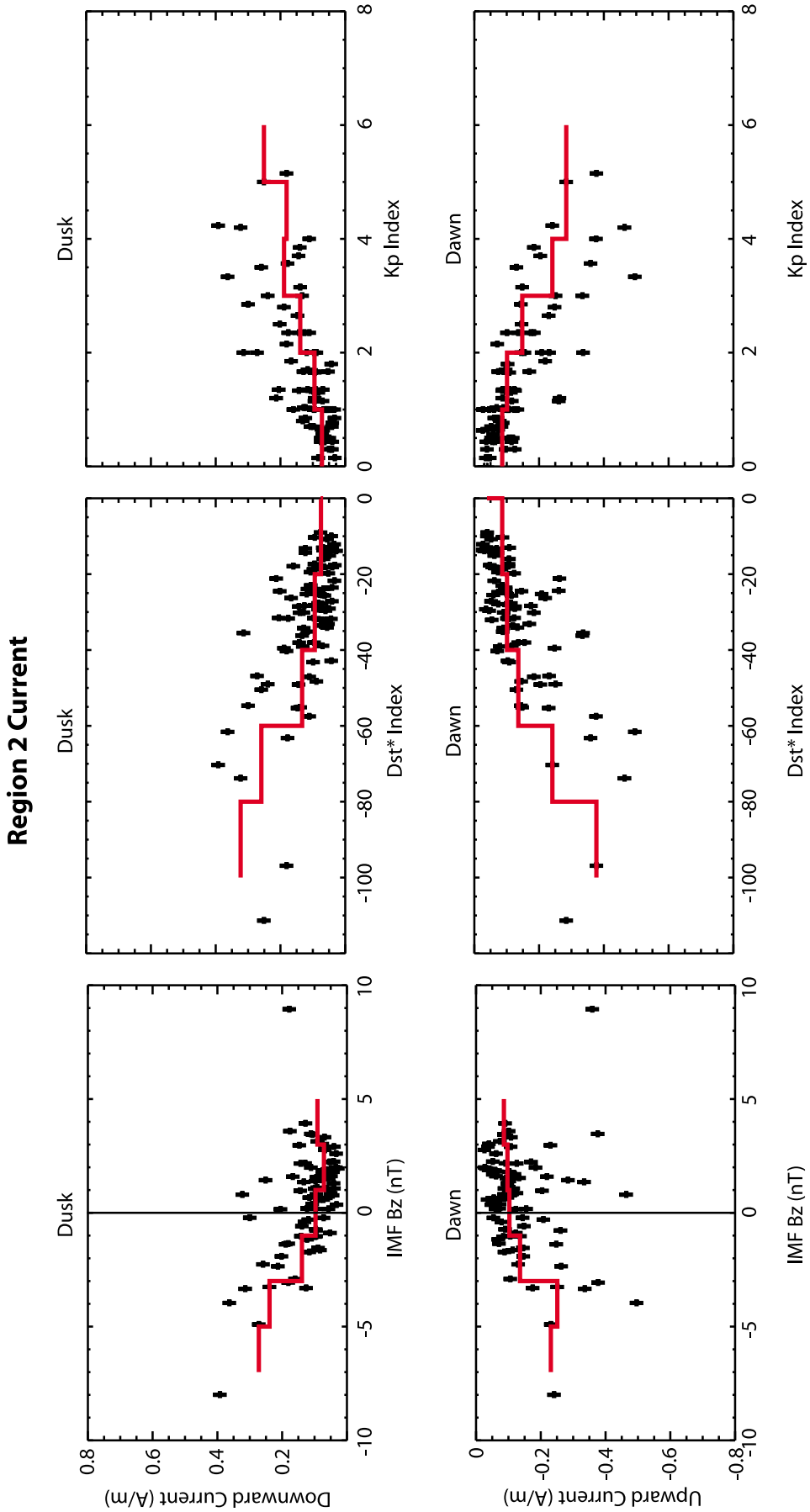

Figure 9. The intensity of the R2 currents as a function of IMF Bz, the Dst* index (the Dst index corrected by the solar wind dynamic pressure), and the Kp index.

intensity during active periods is a secondary effect of enhanced field-aligned currents, since the net currents are a constant percentage of the total R1 field-aligned currents.

4. Summary and Discussions

[23] An unsolved question in the physics of ionosphere-magnetosphere coupling is how field-aligned currents (FACs) close in the ionosphere. In order to maintain the divergence free condition, overall downward FACs (carried mainly by upward electrons) must eventually balance the overall upward FACs associated with the precipitating electrons through ionospheric Petersen currents. Although much of the current closure takes place via local Pedersen currents flowing between the R1 and R2 FACs near the auroral oval, there is a general imbalance, i.e., more currents in R1 than in R2.

[24] In this study, we use the in situ magnetic field observations form ST5 spacecraft to quantify the imbalance of large-scale R1-R2 field-aligned currents. The ST5 data are available during the period from 26 March (near fall equinox) to 24 June 2006 (near winter solstice). The geomagnetic activities during this period are generally from very quiet to moderately active with a few moderate geomagnetic storms. Although we have modeled the large-scale FAC system using an oversimplified geometry and current sheet configuration, the results provide a good indication of the amount of net currents flowing into or out of the ionosphere in the imbalanced R1-R2 current system. We summarize the main results from this study:

[25] 1. If the R1 and R2 currents are imbalanced and there are net FAC currents flowing into or out of the ionosphere, they produce a magnetic field offset over the polar cap. Our observations of the in situ magnetic field across the polar cap show that this is generally the case.

[26] 2. The R1 and R2 current intensities deduced from the in situ magnetic field observations consistently show that the R1 currents are stronger than the R2 currents both for the dawnside and the duskside large-scale FAC system. The net currents flowing into (out of) the ionosphere in the dawnside (duskside) are in the order of 5% of the total R1 currents.

[27] 3. The net currents flowing into or out of the ionosphere are controlled by the solar wind-magnetosphere interaction in the same way as the field-aligned currents themselves are. Our observations show that the net current intensity increases as the magnitude of the IMF Bz component increase during the southward IMF condition but remain unchanged during the northward IMF condition. Due to the same causes, the net currents increases as the Dst* index becomes more negative and/or the Kp index increases. This dependence appears to be a result of the solar wind-magnetosphere interaction. It is a secondary effect due to the enhanced field-aligned currents during periods of enhanced interaction, since the net currents are a percentage of the total field-aligned currents.

[28] Previously, *Iijima and Potemra* [1976] and *Fujii et al.* [1981] reported values of the average current intensity or total currents for the large-scale field-aligned currents using Triad spacecraft. They found that the net currents are in the order of ~20% of the R1 currents on average. *Weimer* [2001] used the in situ magnetic field data from Dynamics Explorer 2 to construct an empirical model of FAC distribution. The total net currents in the empirical model are found to be ~20% of the R1 currents in most cases. More recently, *Christiansen et al.* [2002] reported average parameters of FACs deduced from Ørstead and Magsat data. The net currents they obtained are ~10% of the R1 currents on average and are more pronounced during disturbed conditions. The net currents in all these studies are the difference between the statistically determined average R1 and R2 intensities. They all appear to be stronger than the net currents we obtained from this study, which is ~5% of the R1 currents. Since our results are obtained by obtaining the net currents in each individual case first and then determining the statistically average of the net currents as a percentage of the R1 currents, we believe that our results quantify the cross-polar cap currents more accurately for quiet and moderately active periods. We note that our statistical results are similar to the result of a recent case study by *MacDougall and Jayachandran* [2008]. In this study, ground-based digital ionosonde and magnetometer data from a polar cap station are used to estimate the net currents for a winter case, and it is found that the total net currents are 5% of the R1 currents.

[29] We note that the percentage of ~5% of R1 currents flowing across the polar cap is obtained during generally quiet with occasionally moderately active conditions from near fall equinox to near winter solstice in this study. This percentage may change with seasons and may increase under active conditions as indicated by previous studies [*Iijima and Potemra*, 1976; *Fujii et al.*, 1981, 1994; *Nakano et al.*, 2002; *Nakano and Iyemori*, 2003; *Weimer*, 2001]. This is because the amount the net currents flowing across the polar cap depends on the polar cap electrodynamic parameters such as the conductivity and the electric field. The ratio of the across-polar cap Pedersen currents to the auroral zone Pederson currents is correlated to the ratio of the polar cap conductivity to the auroral zone conductivity. The polar cap conductivity produced mainly by solar EUV flux and changes considerably with seasons [*Moen and Brekke*, 1993]. The auroral zone conductivity depends on both the solar EUV flux and auroral particle precipitations [*Robinson et al.*, 1985]. It is an important topic in future studies to evaluate how the percentage of the R1 currents that flow across the polar cap changes with geomagnetic conditions, especially during extreme space weather conditions.

[30] The closure path of the net currents due to the imbalance of the R1 and R2 currents is an important question, because it is related to the questions where Pedersen currents flow and where Joule dissipations occur in the ionosphere. Field-aligned currents close in the ionosphere as Pedersen currents. The portion of the R1 currents that balances the R2 currents is closed by Pedersen currents flowing within the R1-R2 pair in the auroral zone. These Pedersen currents at the auroral zone provide a $\mathbf{J} \times \mathbf{B}$ force to drive sunward ionospheric plasma convection at and below the auroral zone latitudes, i.e., to move the plasma flow sunward against the fictional force due to ion-neutral collisions [*Strangeway et al.*, 2000]. Since large-scale electric fields generated from a combination of viscous interactions and magnetic reconnection processes at the magnetopause map into the high-latitude ionosphere, measured as the cross-polar cap potential, there must be cross-polar cap Pederson currents flowing along the electric fields unless the polar cap

has zero conductivity. The cross-polar cap Pedersen currents provide driving force for the tailward (or antisunward) plasma convection over the polar cap. Thus, the net currents due to the imbalance of the R1 and R2 currents require that their closure currents flow across the polar cap from dawn to dusk as Pedersen currents. *Kikuchi et al.* [1996] proposed an equatorial closure path for the FACs during geomagnetic storms, in which the R1 and R2 currents flow into the dayside equatorial ionosphere and drive the equatorial DP2 currents and counter electrojet. However, we believe that the dominant mechanism for the closure of the R1-R2 FAC imbalance is through the cross-polar cap Pedersen currents, as they are required for the ionospheric plasma convection in the polar cap.

[31] Although the cross-polar cap Pedersen currents are only a small fraction of the R1 currents, they still represent a significant amount of Pedersen currents flowing across the polar cap. Previous observations have determined that the total R1 currents are in the order of a few MA, comparable to the total amount of Chapman-Ferraro current in the magnetopause [e.g., *Midgley and Davis*, 1963] and the ring current in the inner magnetosphere [e.g., *Le et al.*, 2004]. Thus, the total amount of the cross-polar cap Pedersen currents is in the order of ~0.1 MA. Our statistics also shows that the total amount of currents is correlated with the geomagnetic indices and the IMF Bz component during the southward IMF conditions. This result is consistent with the previous results by *Christiansen et al.* [2002], in which the net currents are stronger during disturbed times, and by *Weimer* [2001], who found that the total cross-polar cap Pedersen currents vary from ~0.1 MA at 50 kV polar cap potential to ~0.5 MA at 120 kV. Our results are also consistent with high-latitude observations that the integrated Joule heating increases with IMF magnitude when the IMF is southward [*Weimer*, 2005] but relatively unchanged when the IMF is northward [*McHarg et al.*, 2005]. Since the total amount of the R1 and R2 currents are similarly controlled by these parameters [*Zanetti and Potemra*, 1986], we believe the dependence of the net currents on the IMF and the geomagnetic indices obtained in our study appears to be a secondary effect of the control of the R1-R2 currents by the solar wind-magnetosphere interaction under the quiet and moderately active conditions.

[32] It is well known that Joule heating or frictional heating due to Pedersen currents is a high-latitude ionospheric phenomenon, in which the ion drift energy is turned into the thermal energy and kinetic energy of neutrals through collisions. Previous observations have showed that the spatial distribution of the Joule heating spreads over a larger magnetic latitude range into the polar cap [*Olsson et al.*, 2004; *Palmroth et al.*, 2004] and there is evidence that the Joule heating occurs throughout the polar cap region (D. J. Knipp, private communications). These observations are consistent to ours that Pedersen currents close the imbalanced portion of the R1-R2 currents by flowing across the polar cap from dawn to dusk. Despite the fact that the R1-R2 imbalance only contributes ~5% of the total R1 currents to the cross-polar cap Pedersen currents whereas ~95% flow as auroral zone Pedersen currents, the integrated Joule heating rate will have a much larger percentage due to the much larger area of the polar cap. Hence, the energy dissipation in the polar cap cannot be ignored. *Palmroth et al.* [2004] found that the Joule heating power in the polar cap could reach as high as ~50% of the value in the aural zone during geomagnetic storms and substorms in their global MHD simulations of ionospheric energy inputs. Given the importance of the Joule heating to the high-latitude ionospheric electrodynamics, quantifying the cross-polar cap Pedersen currents and associated Joule heating is needed for developing models of the magnetosphere-ionosphere coupling. This study, although with a very limited data set, is an attempt to understand and quantify these currents. However, we still do not have a good knowledge on how the cross-polar cap currents vary with seasons, hemisphere, solar irradiance, ionospheric conductivity, and solar wind conditions. Further work using a large data base is required to quantify the cross-polar cap Pedersen currents under various conditions.

5. Conclusion

[33] In this study, we use the in situ magnetic field observations from Space Technology 5 mission to quantify the imbalance of R1 and R2 currents. We have consistently observed the magnetic field offsets produced by the imbalanced R1-R2 currents. The R1 current intensities deduced from the magnetic field observations are consistently stronger than the R2 current intensity both for the dawnside and the duskside large-scale FAC system. The net currents flowing into (out of) the ionosphere in the dawnside (duskside) are in the order of 5% of the total R1 currents. We also find that the net currents flowing into or out of the ionosphere are correlated with geomagnetic indices and controlled by the solar wind-magnetosphere interaction in the same way as the field-aligned currents themselves are. Since the net currents due to the imbalance of the R1 and R2 currents require that their closure currents flow across the polar cap from dawn to dusk as Pedersen currents, our results indicate that the total amount of the cross-polar cap Pedersen currents is in the order of ~0.1 MA. This study, although with a very limited data set, is one of a few attempts to quantify the cross-polar cap Pedersen currents. Given the importance of the Joule heating due to Pedersen currents to the high-latitude ionospheric electrodynamics, quantifying the cross-polar cap Pedersen currents and associated Joule heating is needed for developing models of the magnetosphere-ionosphere coupling.

[34] **Acknowledgment.** Robert Lysak thanks the reviewers for their assistance in evaluating this paper.

References

Banks, P., J. Foster, and J. Doupnik (1981), Chatanika radar observations relating to the latitudinal and local time variations of joule heating, *J. Geophys. Res.*, *86*(A8), 6869–6878.

Burton, R. K., R. L. Mc Pherron, C. T. Russell (1975), The terrestrial magnetosphere: A half-wave rectifier of the interplanetary electric field, *Science*, *189*, 717–718.

Chappell, C., T. Moore, and J. Waite Jr. (1987), The ionosphere as a fully adequate source of plasma for the Earth's magnetosphere, *J. Geophys. Res.*, *92*(A6), 5896–5910.

Christiansen, F., V. O. Papitashvili, and T. Neubert (2002), Seasonal variations of high-latitude field-aligned currents inferred from Ørsted and Magsat observations, *J. Geophys. Res.*, *107*(A2), 1029, doi:10.1029/2001JA900104.

Fujii, R., and T. Iijima (1987), Control of the ionospheric conductivities on large-scale Birkeland current intensities under geomagnetic quiet conditions, *J. Geophys. Res.*, *92*(A5), 4505–4513.

Fujii, R., T. Iijima, T. Potemra, and M. Sugiura (1981), Seasonal dependence of large-scale Birkeland currents, *Geophys. Res. Lett.*, *8*(10), 1103–1106.

Fujii, R., R. A. Hoffman, P. C. Anderson, J. D. Craven, M. Sugiura, L. A. Frank, and N. C. Maynard (1994), Electrodynamic parameters in the nighttime sector during auroral substorms, *J. Geophys. Res.*, *99*(A4), 6093–6112.

Fujii, R., S. Nozawa, S. Buchert, and A. Brekke (1999), Statistical characteristics of electromagnetic energy transfer between the magnetosphere, the ionosphere, and the thermosphere, *J. Geophys. Res.*, *104*(A2), 2357–2365.

Fukushima, N. (1976), A generalized theorem of no groung magnetic effect of vertical current connected with Pedersen currents in the uniform conductivity ionosphere, *Rep. Ionos. Space Res. Jap.*, *30*, 35–50.

Gary, J., R. Heelis, W. Hanson, and J. Slavin (1994), Field-aligned poynting flux observations in the high-latitude ionosphere, *J. Geophys. Res.*, *99*(A6), 11417–11427.

Iijima, T., and T. Potemra (1976), The amplitude distribution of field-aligned currents at northern high latitudes observed by Triad, *J. Geophys. Res.*, *81*(13), 2165–2174.

Kikuchi, T., H. Lühr, T. Kitamura, O. Saka, and K. Schlegel (1996), Direct penetration of the polar electric field to the equator during a DP 2 event as detected by the auroral and equatorial magnetometer chains and the EISCAT radar, *J. Geophys. Res.*, *101*(A8), 17161–17173.

Le, G., C. T. Russell, and K. Takahashi (2004), Morphology of the ring current derived from in situ magnetic field measurements, *Ann. Geophys.*, *22*, 1267–1295.

Le, G., Y. Wang, J. A. Slavin, R. J. Strangeway (2009), Space Technology 5 multipoint observations of temporal and spatial variability of field-aligned currents, *J. Geophys. Res.*, *114*, A08206, doi:10.1029/2009JA014081.

Lu, G., A. Richmond, B. Emery, and R. Roble (1995), Magnetosphere-ionosphere-thermosphere coupling: Effect of neutral winds on energy transfer and field-aligned current, *J. Geophys. Res.*, *100*(A10), 19643–19659.

Lu, G., et al. (1998), Global energy deposition during the January 1997 magnetic cloud event, *J. Geophys. Res.*, *103*(A6), 11685–11694.

MacDougall, J., and P. T. Jayachandran (2008), Winter cross-polar cap current estimation, *Adv. Space Res.*, *42*,797–801.

McHarg, M., F. Chun, D. Knipp, G. Lu, B. Emery, A. Ridley (2005), High-latitude Joule heating response to IMF inputs, *J. Geophys. Res.*, *110*, A08309, doi:10.1029/2004JA010949.

Midgley, J. E., and L. Davis Jr. (1963), Calculation by a moment technique of the perturbation of the geomagnetic field by the solar wind, *J. Geophys. Res. 68*, 5111–5123.

Moen, J., and A. Brekke (1993), The solar flux influence on quiet time conductances in the auroral ionosphere, *Geophys. Res. Lett.*, *20*(10), 971–974.

Nakano, S., and T. Iyemori (2003), Local time distribution of net field-aligned currents derived from high-altitude satellite data, *J. Geophys. Res.*, *108*(A8), 1314, doi:10.1029/2002JA009519.

Nakano, S., T. Iyemori, and S. Yamashita (2002), Net field-aligned currents controlled by the polar ionospheric conductivity, *J. Geophys. Res.*, *107*(A5), 1056, doi:10.1029/2001JA900177.

Olsson, A., P. Janhunen, T. Karlsson, N. Ivchenko, and L. G. Blomberg (2004), Statistics of Joule heating in the auroral zone and polar cap using Astrid-2 satellite Poynting flux, *Ann. Geophys.*, *22*, 4133–4142.

Palmroth, M., P. Janhunen, T. I. Pulkkinen, and H. E. J. Koskinen (2004), Ionospheric energy input as a function of solar wind parameters: global MHD simulation results, *Ann. Geophys.*, *22*, 549–566.

Robinson, R., R. Vondrak, and T. Potemra (1985), Auroral Zone Conductivities within the Field-Aligned Current Sheets, *J. Geophys. Res.*, *90*(A10), 9688–9696.

Slavin, J. A., G. Le, R. J. Strangeway, Y. Wang, S. A. Boardsen, M. B. Moldwin, and H. E. Spence (2008), Space Technology 5 multi-point measurements of near-Earth magnetic fields: Initial results, *Geophys. Res. Lett.*, *35*, L02107, doi:10.1029/2007GL031728.

Stauning, P., and F. Primdahl (2000), First detection of global dawn-dusk ionospheric current intensities using Ampère's integral law on Ørsted orbits, *Geophys. Res. Lett.*, *27*(20), 3273–3276.

Strangeway, R., C. Russell, C. Carlson, J. McFadden, R. Ergun, M. Temerin, D. Klumpar, W. Peterson, and T. Moore (2000), Cusp field-aligned currents and ion outflows, *J. Geophys. Res.*, *105*(A9), 21129–21141.

Sugiura, M., and T. Potemra (1976), Net Field-Aligned Currents Observed by Triad, *J. Geophys. Res.*, *81*(13), 2155–2164.

Weimer, D. (2001), Maps of ionospheric field-aligned currents as a function of the interplanetary magnetic field derived from Dynamics Explorer 2 data, *J. Geophys. Res.*, *106*(A7), 12,889–12,902.

Weimer, D. R. (2005), Improved ionospheric electrodynamic models and application to calculating Joule heating rates, *J. Geophys. Res.*, *110*, A05306, doi:10.1029/2004JA010884.

Yau, A. W., and M. Andre (1997), Sources of ion outflow in the high latitude ionosphere, *Space Sci. Rev.*, *80*, 1–25.

Zanetti, L. J., and T. A. Potemra (1986), The relationship of Birkeland and ionospheric current systems to the interplanetary magnetic field, in *Solar Wind-Magnetosphere Coupling*, edited by Y. Kamide and J. A. Slavin, pp. 547–562, Terra Sci. Pub. Co., Tokyo.

Zheng, Y., T. E. Moore, F. S. Mozer, C. T. Russell, R. J. Strangeway (2005), Polar study of ionospheric ion outflow versus energy input, *J. Geophys. Res.*, *110*, A07210, doi:10.1029/2004JA010995.

G. Le and J. A. Slavin, Mail Code 674, NASA Goddard Space Flight Center, Greenbelt, MD 20771, USA. (Guan.Le@nasa.gov)

R. J. Strangeway, Institute of Geophysics and Planetary Physics, University of California, Los Angeles, CA 90095, USA.